Application of Co–Ni–P Coating on Grain-Oriented Electrical Steel

[1]Pabitra Rout[2] Chandan Kumar Nayak [3]Bipasha Mohapatra [4]Manmath Das
Gandhi Institute for Technology, Bhubaneswar

An electroless plating of Co–Ni–P was applied to a grain-oriented electrical steel substrate, resulting in a power loss improvement of 9%–11%. The mean thickness of the coating was found to be 2.15 0.15 μm from environmental scanning electron microscopy images. Shifts of the magnetostriction stress sensitivity curves showed that stress was acting on the substrate and was corroborated by a shift in X-ray diffraction (XRD) peaks and narrowing of the domains after the samples were coated. The magnetic property measurement system results confirmed the magnetic nature of the coating and XRD results showed peaks of α-iron in the uncoated sample, α-iron-cobalt and α-iron in the Co-Ni-P-coated sample. The Talysurf profilometer showed a decrease in surface roughness values after coating the sample, which reduced the hysteresis loss.

***Index Terms*— Electroless coating, grain-oriented electrical steel, magnetic coating, magnetostriction, power loss, stress.**

I. Introduction

EFFORTS are being made to produce high-performance electrical steel through several methods, including better secondary recrystallization methods [1], grain orientation control [2], increasing the electrical resistivity, gauge reduction [3], and understanding the magnetic domain structure [4]–[7]. Perhaps the greatest gains can be obtained by employing effective stress coatings [8], [9], which can play a dominant role in minimizing losses and magnetostriction.

Stress can be applied to the material with the help of coatings. Coating the steel helps in reducing both the losses and the magnetostriction. It is well known that the effect of magnetostriction can be suppressed by the application of tensile stresses. Tensile stress imparted from the coating on the steel sheet eliminates the surface closure domains, and losses are reduced as tensile stress helps in narrowing the domain-wall spacing in addition to minimizing the circulation of eddy currents by providing electrical insulation. Current coating systems on grain-oriented electrical steel comprise a two-layer coating with a forsterite layer (Mg_2SiO_4) below an aluminum orthophosphate layer. Conventionally, coatings that have low coefficient of thermal expansion are used, because when cooled from high temperature, they contract lesser than does the substrate. This difference in cooling applies a tensile stress on the substrate.

A number of different methods can be used to apply a coating on the surface of a steel sheet such as sol–gel [10], chemical vapor deposition [11], physical vapor deposition [12], plasma spraying, wet coating, printing, electroless plating, and electrochemical method.

This paper investigates electroless plating of Co–Ni–P, which has the advantages of corrosion resistance, uniform

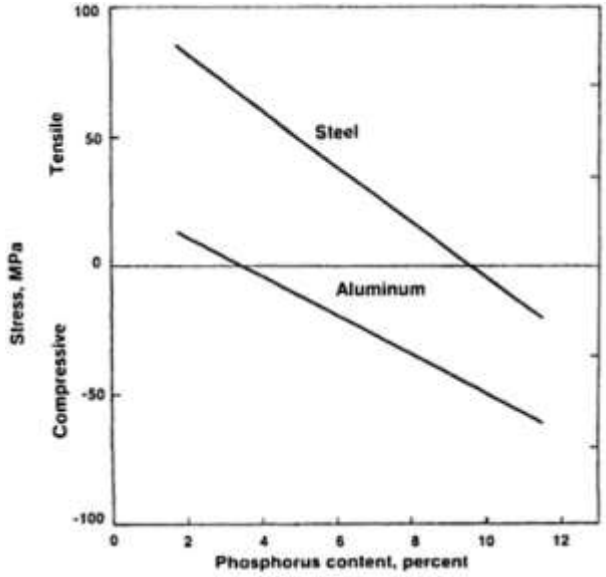

Fig. 1. Relationship between phosphorus content and stress in the coating.

thickness, and wear and abrasion resistance. Stress develops in electroless plating due to the difference in the coefficient of thermal expansion between the substrate and the coating or develops in the deposition process. During deposition, the particles get deposited at a few places rather than forming a uniform atomic layer. The coating grows at those few places only. Surface tension binds the particles together. Rearrangement of these atoms due to surface tension changes the interatomic distance and hence develops tensile or compressive stress depending on the increase or decrease in the interatomic distance. Minimizing the coagulation could reduce the amount of tensile stress, and by introducing phosphorus, the stress can be changed from tensile to compressive, as can be seen in Fig. 1 [13]. The electroless deposition rates are very fast as compared with other chemical coating techniques, and being autocatalytic, no external current is supplied for the process to take place.

Chivavibul *et al.* [14] produced an electroless Ni–Co–P coating of 1 μm thickness on non-oriented electrical steel and found that the coating was effective in reducing losses by up to 4% at a magnetic flux density of 0.3 T and frequency of 400 Hz. The coating was able to minimize the eddy current loss at higher frequencies to reduce the overall loss. Power transformers operate at a flux density of 1.5 T and above and a frequency of 50 Hz. The component of eddy current loss decreases as the frequency decreases. It was also found that as the thickness of Ni–Co–P coating increased, hysteresis loss increased and hence Ni–Co–P may not be suitable at lower frequencies, where hysteresis and anomalous loss dominate [15]. Co–Ni–P was chosen as a suitable coating. The amount of phosphorus could be balanced to develop compressive stress in the coating. The coating is also ferromagnetic, and its properties can be altered by varying the chemical content. The parameters used to deposit the Co–Ni–P coating determine the impact on final magnetic properties such as the coercivity and hysteresis loss [16]. The aim of this paper is to evaluate and optimize these coatings for transformer applications and compare them with conventional coatings.

II. Material and Methods

Grain-oriented (Fe-3%Si) samples (0.3 mm $\times$ 30 mm $\times$ 305 mm) were supplied by Cogent Power Ltd., Newport, and both the tension and insulation coating were removed with a solution of 7.5% sulphuric acid and 1% hydrofluoric acid for approximately 10 min and then in 4% nitric acid for approximately 7 min. The specific total loss was measured with a single strip tester [17] from a magnetic flux density of 1.1 T to 1.7 T at a frequency of 50 Hz. Flux closure was provided by a pair of high permeability wound yokes with a 255 mm pole gap, and the number of turns on the primary and secondary windings was 865 and 250, respectively. A mutual inductor was used to provide air flux compensation. The magnetostriction measurements were made on a magnetostriction measurement system using the procedure described in [18]. The stress induced by the coating was also calculated from the measured magnetostriction curves using the method outlined in [18]. The microscopy images were obtained from an XL30 ESEM field emission gun. The elemental analysis was performed with an Oxford Instruments energy-dispersive X-ray spectroscopy (EDX) analysis system. To study the structure and phases of the coating, X-ray diffraction (XRD) was carried out, with cobalt radiation at 30 kV and 40 mA. The magnetic domains were imaged with a magnetic pattern viewer [19]. The magnetic properties of the coating were measured at room temperature by the magnetic property measurement system (MPMS). The magnetic field was applied up to 20 000 Oe. The surface roughness of the uncoated and coated surfaces was measured by Talysurf surface profilometer. The measurement was made in the direction of rolling for a distance of 40 mm for all the samples. The samples were coated with Co–Ni–P using electroless plating. The composition of the bath and the operating conditions was referred from [20] and modified as shown in Table I. To study the effect of coating thickness on the substrate, four samples were immersed in the plating solution and were removed at 20, 35, 50, and 90 min, respectively. The pH of the solution was maintained by adding ammonium hydroxide. To ascertain the effect of pH on the power loss, five samples were prepared with pH values varying from 7.8 to 9.4. All five samples were immersed for 90 min, as it was found to be the optimum time for best results.

TABLE I
Electroless Plating Bath Conditions

Composition	Grams/litre
Nickel sulphate	7.5
Cobalt sulphate	15
Trisodium citrate	50
Sodium hypophosphite	25
Boric acid	30
Temperature 60 ± °5	

III. Results and Discussion

A. Power Loss Results for Various Thicknesses

Fig. 2 shows the difference in power loss of the coated and uncoated samples for different times. The uncoated power loss was different for different strips because the Epstein strips cut from a sheet material show a significant local variation in grain size, orientation, and pinning sites. The thickness of the coating deposited was proportional to the time for which the samples were kept in the plating solution. The dehydrogenation of hypophosphite provides the hydride ion (1a). The deposition of nickel and cobalt on the surface of grain-oriented electrical steel was triggered by the reduction of nickel and cobalt ions by the hydride ion as shown in reactions (1b) and (1c) [21]. These deposited particles act as nucleation sites for further deposition of coating and hence the time period of coating dictates the thickness of coating deposited

$$H_2PO_2^- + H_2O \rightarrow H^+ + HPO_3^{2-} + 2H \quad (1a)$$

$$Ni^{2+} + 2H \rightarrow Ni^0 + 2H^+ \quad (1b)$$

$$Co^{2+} + 2H \rightarrow Co^0 + 2H^+. \quad (1c)$$

Fig. 2(a)–(d) shows that the coating thickness plays a major role in determining the power loss with a thicker coating applying greater stress. For the sample coated for 20 min, the reduction in power loss was around 4%–5%. Material coated for 90 min had a reduction in loss of approximately 9%–11% at 1.5 T as compared with the uncoated sample. The values of stress calculated for 20 and 90 min coated samples were 0.86 and 2.10 MPa, respectively. Song and Yu [22] showed that stress was introduced to the substrate by the Ni–P coating, The stress can be tensile or compressive depending upon the amount of phosphorus in the coating; 8.5% phosphorus induces compressive stress in the coating [23]. The phosphorus gets trapped during the deposition and forms small grains monodomains, increasing the soft magnetic properties [24]. In this case, the stress in the coating was compressive as the amount of phosphorus was confirmed to be between 9% and 10%, and hence tensile stress acted on the substrate, which was

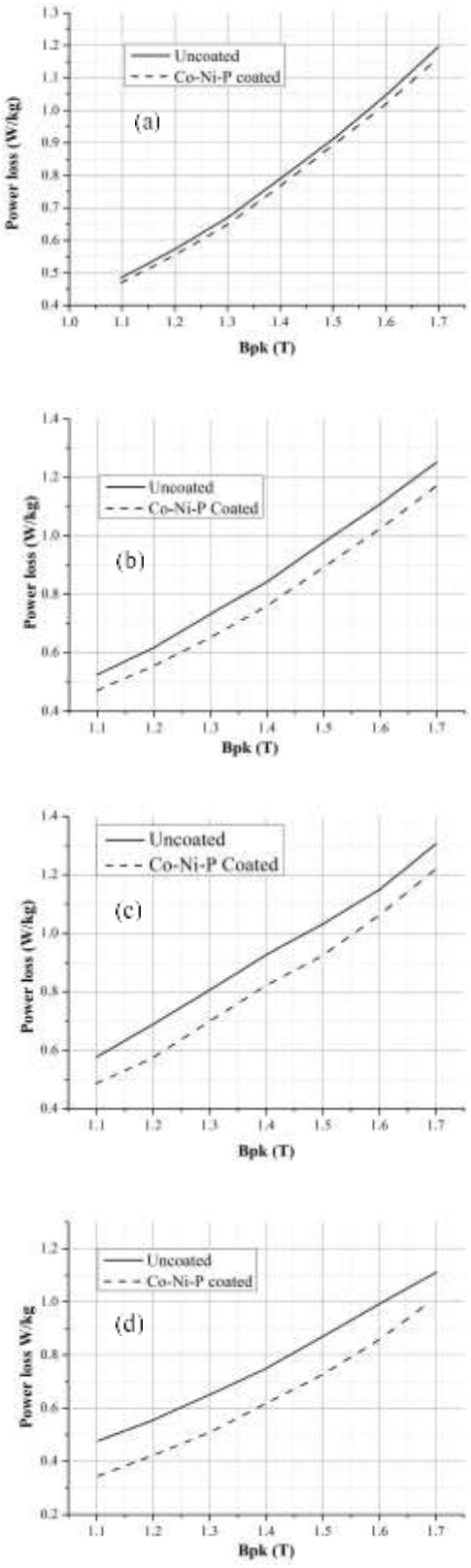

Fig. 2. Power loss testing for the uncoated and Co–Ni–P-coated samples for different times. (a) 20 min. (b) 35 min. (c) 50 min. (d) 90 min.

beneficial in terms of power loss reduction and magnetostriction. To minimize losses, coating thickness could be increased, but the stress decreases as the thickness increases [23] and

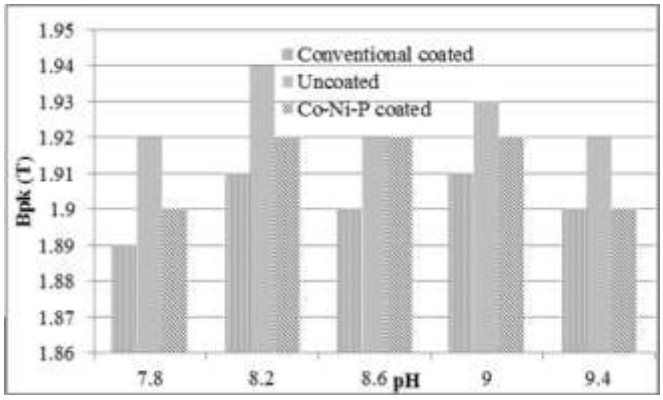

Fig. 3. Bpk measured at magnetic field strength of 800 A/m for different values of pH.

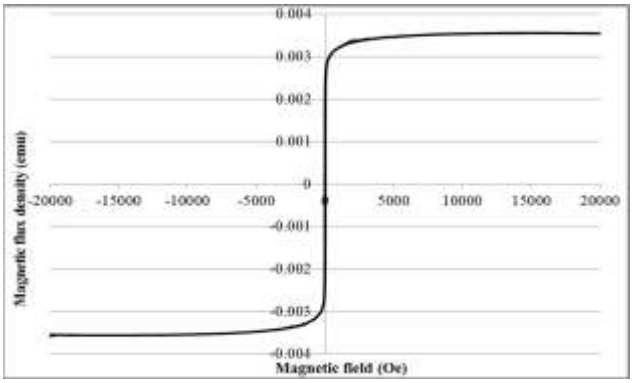

Fig. 4. Magnetic flux density measured for Co–Ni–P coated at pH 9.0.

it leads to unacceptable degradation of permeability shown in Fig. 3, where the Bpk (magnetic flux density at 800 A/m magnetic induction) was reduced after coating, and stacking factor gets affected.

B. Magnetic Properties

Fig. 4 shows a classical hysteresis loop for Co–Ni–P coating at pH 9.0. The *B–H* loop measured by the MPMS validates the magnetic nature of the coating. The coercivity of the coating was calculated to be 796 A/m. The saturation magnetization of the coating was calculated to be 0.0036 emu as compared with 0.0288 emu for grain-oriented electrical steel, considering same volume for both materials. The magnetic property of Co–Ni–P coating increases the stacking factor by adding a soft magnetic material in the transformer core as compared with the conventional non-magnetic coating.

C. Magnetostriction

Fig. 5 shows the magnetostriction curve for the uncoated and Co–Ni–P-coated samples for 90 min at pH 9.0. The threshold (point-of-zero magnetostriction) for the uncoated and Co–Ni–P-coated samples was around 1 and 3 MPa, respectively. A stress shift of 1.80 ± 0.20 MPa was observed after coating the sample. This shift in the magnetostriction curve toward the left infers that a significant amount of stress

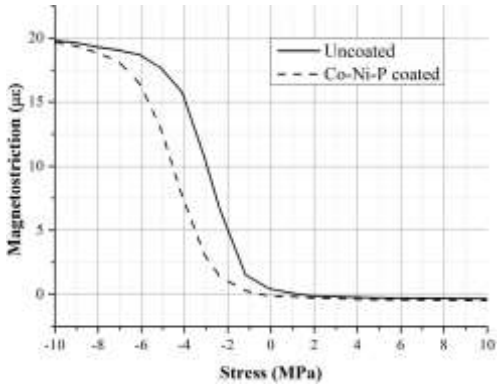

Fig. 5. Magnetostriction versus stress for uncoated and Co–Ni–P coated for 90 min.

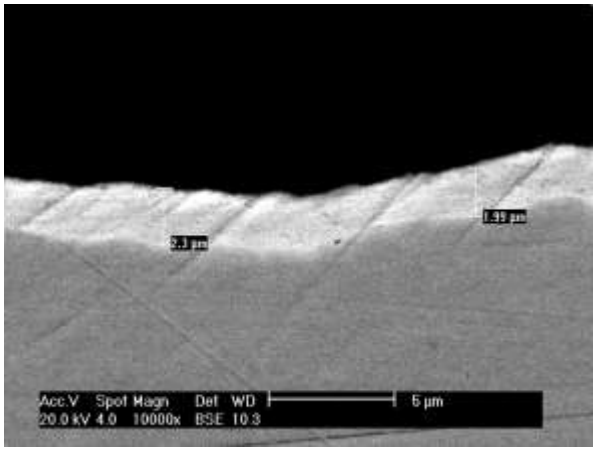

Fig. 6. Cross-sectional image of the substrate and the coating at pH 9.

was acting on the substrate. Applying a compressive coating on the substrate eliminates the surface closure domains. These surface closure domains are responsible for magnetostriction [18]. As the surface closure domains are minimized, the magnetostriction reduces.

D. Scanning Electron Microscopy

Fig. 6 shows the scanning electron microscopy (SEM) image of the 90 min coated sample at pH 9. The gray area shows the substrate, while the lighter area shows the coating. The coating was uniformly distributed across the sample. No gaps or cracks were found. The thickness of the coating was averaged to be around 2.15 $\pm$0.15 μm.

The stacking factor calculated for 2 μm-thick coating was 98.68%, as compared with 97.4% for 4 μm-thick conventional coating calculated as

$$\text{stacking factor} = 1 - \frac{\text{Non-magnetic material in the core}}{\text{Total material in the transformer}} * 100 .$$

If the coating was non-magnetic, the thickness of coating on both sides was 4 μm.

The thickness of Epstein strip without coating = 300 μm.

The thickness of total material in the transformer core = 304 μm

$$\text{stacking factor}(\%) = 1 - \frac{300}{304} * 100$$

$$\text{stacking factor}(\%) = 98.68.$$

However, as the coating was also magnetic, it would contribute to the stacking factor, and hence the new value of stacking factor considering the saturation magnetization of Co–Ni–P coating to be 0.0036 emu and that of GOES to be 0.0288 emu was 98.84%. The increase in stacking factor by the magnetic nature of the coating was found to be insignificant

$$\text{Magnetic contribution of coating to GOES} = \frac{0.0036}{0.0288} * 100$$

$$\text{Magnetic contribution of coating to GOES} = 12.5\%$$

$$\text{New stacking factor}(\%) \quad 98.68 \quad \frac{100 - 98.68}{100} * 12.5$$

$$\text{New stacking factor}(\%) = 98.84.$$

Fig. 7 shows five SEM images of the samples prepared with coating at various pH values (7.8, 8.2, 8.6, 9, and 9.4). pH plays a major role in determining the type of coating (hard or soft magnetic) and controls the coating mechanism [25]. At pH 1.5, the coating was found to be having a coercivity of 11, 937 A/m and at pH 3.5, value the coating had a coercivity of 47, 747 A/m [24], [26]. As can be seen from the images at a pH of 7.8, the Co–Ni–P coating coagulates in some areas rather than forming a uniform coating. The nucleation of Ni and Co on the surface of grain-oriented electrical steel is not distributed throughout the sample; instead the metal particles nucleate at a few sites. The coating grows at those sites only. The surface tension binds the particle together and changes the interatomic spacing. The change in interatomic spacing introduces tensile or compressive stress in the coating [13]. A reduction in interatomic spacing would lead to a compressive stress in the coating and therefore a tensile stress in the substrate. As the pH of the solution was increased, there was a reduction in size of the particles and a more uniform coating was formed. At pH 9, nucleation occurs throughout the sample and we could see a uniform coating on the substrate and a minimal amount of coagulation in the coating. The stress applied by the coating on the substrate was uniform and a reduction in power loss was observed. The pH was increased further and the coating was again found to be coagulated at various places.

E. Surface Profiling

The surface roughness values in Fig. 8 validate the SEM results. The value of roughness was largely dependent on the pH of the coating solution. The surface of the sample coated with a pH value of 7.8 was found to be rougher than the uncoated sample. The least value of roughness was measured at a pH of 9.0. The surface roughness effects the hysteresis loss [27]. The increase in surface roughness increases the number of free poles on the surface, and these free poles pin the domain walls. It leads to reduction of domains, and the motion of domain wall is inhomogeneous [9]. Energy is

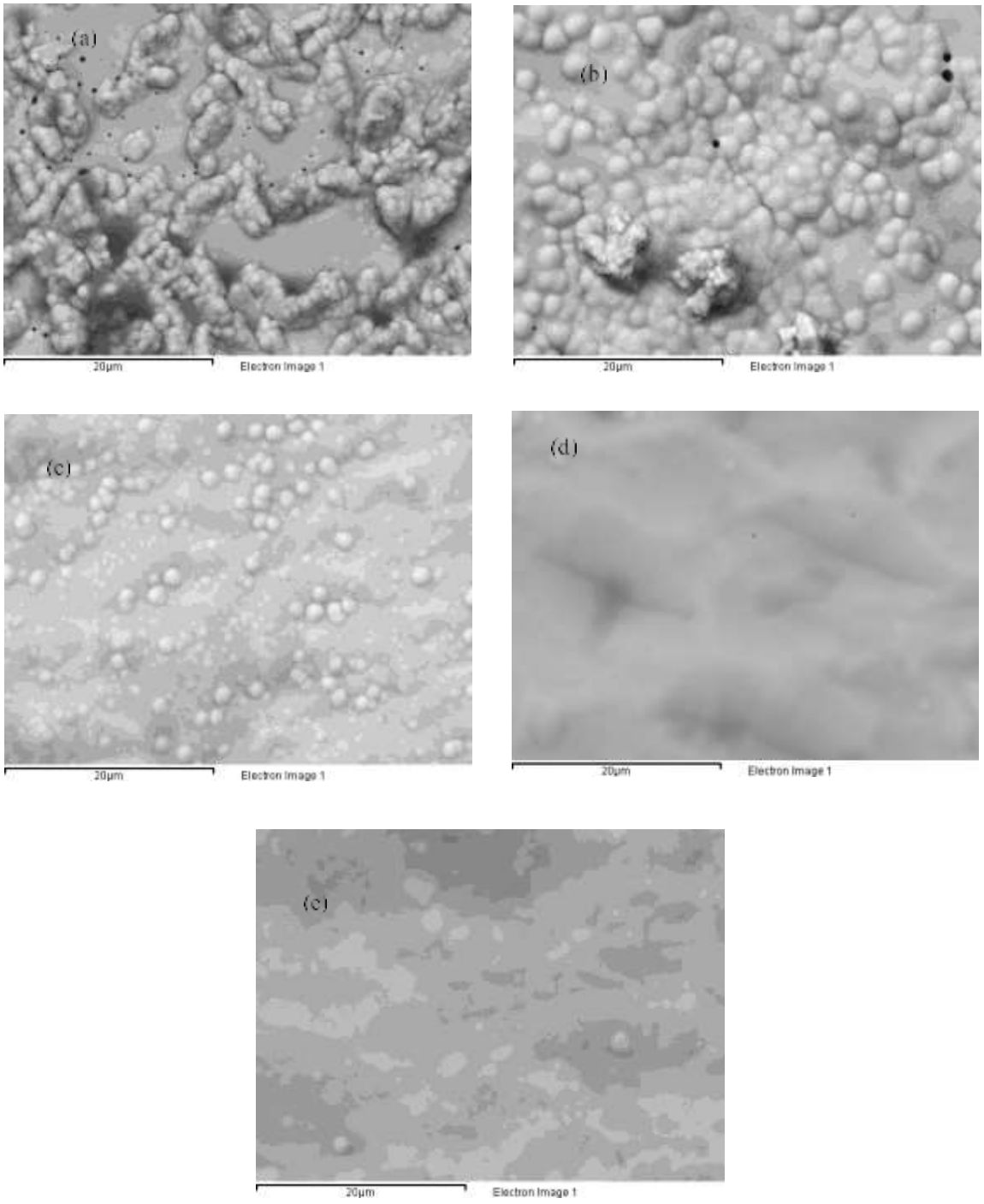

Fig. 7. SEM images for the samples coated with different pH values. (a) 7.8. (b) 8.2. (c) 8.6. (d) 9. (e) 9.4.

dissipated in freeing these domain walls, and this energy contributes to specific total loss. It was assumed that the enhancement of magnetic properties at pH 9.0 was due to the improvement in surface roughness by magnetically active coating.

F. Effect of pH on Coating Composition and Power Loss

Fig. 9 shows the power loss results of the different samples. As expected and endorsed by the SEM images, the sample coated at a pH of 9 shows the highest reduction in power loss, because a uniform coating could be achieved only at this value. Changing the pH value either way affects the coating formation, which generates tensile stress in the coating and the improvement in power loss reduction gets reduced. Table II highlights the elements present in the coating at different pH values. The cobalt content in the coating increased as the pH was increased and reached a maximum of 60%–62% by weight for a pH of 9. On the other hand,

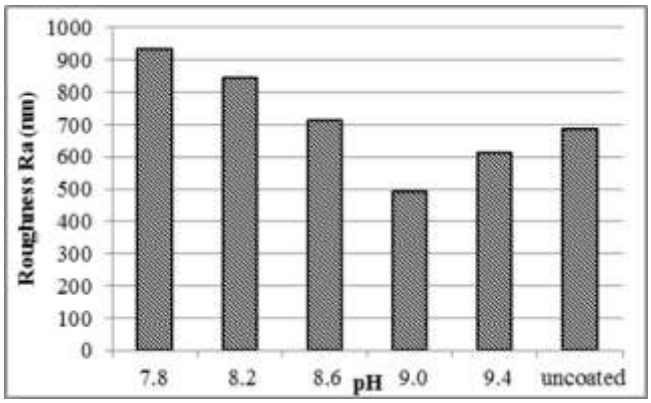

Fig. 8. Talysurf surface roughness values Co–Ni–P coating at different pH values.

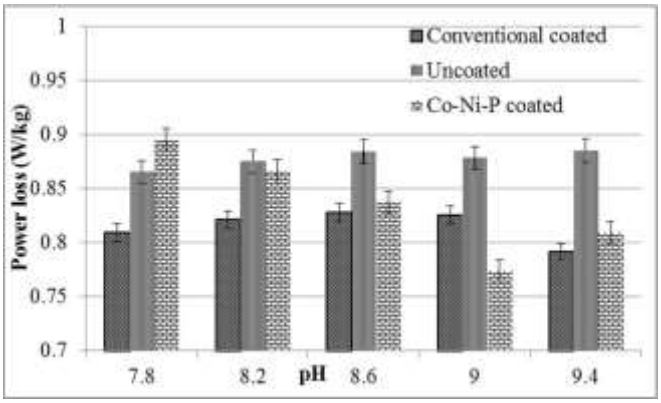

Fig. 9. Effect of pH on power loss measured at 1.5 T and 50 Hz frequency.

nickel content decreased. The results were in agreement with [26]. The saturation magnetization of cobalt (167 emu/g) was much higher than that of nickel (54 emu/g), and so, increasing cobalt content would result in better soft magnetic properties. The amount of phosphorus remains relatively unchanged except for the coating with a pH of 9.4 where sodium was introduced in the coating, and the compressive stress from the coating reduces, which may be the reason for the decrease in improvement of power loss at a pH value of 9.4.

G. Magnetic Domain Imaging and Loss Separation

To study the effect of coating on power loss, the domain images were recorded before and after coating the sample. The magnetic domain imaging clearly shows the narrowing of domains after coating with Co–Ni–P. The average domain width in the rectangular box in Fig. 10 for the uncoated sample was 0.73 mm as compared with 0.48 mm for the Co–Ni–P-coated sample. The narrowing of domain width decreases the anomalous loss. The anomalous loss is directly proportional to velocity of the domain wall. As the domain width decreases, the walls have to travel a shorter distance within the same time, so the velocity of the wall decreases [5].

The model used here for loss separation was proposed in [15]. The core loss equation is

$$W = k_h f B^{\alpha} + k_e f^2 B^2 + K_a f^{1.5} B^{1.5} \quad (2a)$$

TABLE II
ELEMENTAL COMPOSITION (WEIGHT%) OF COATING AT DIFFERENT pH VALUES

pH	Nickel%	Cobalt%	Phosphorus%	Sodium%
7.8	41-43	48-50	9-10	0
8.2	33-35	54-56	9-10	0
8.6	32-34	55-57	9-10	0
9.0	29-31	60--62	9-10	0
9.4	28-30	58-60	7-8	4-5

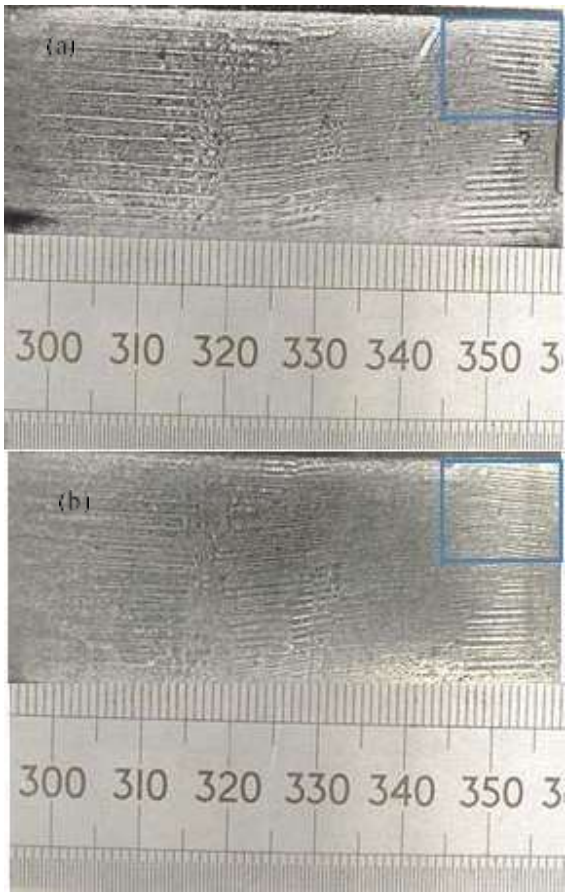

Fig. 10. Magnetic domain imaging for the (a) uncoated and (b) Co–Ni–P-coated samples at pH 9.

where W is the total loss, $k_h f B^{\alpha}$ is the hysteresis loss component, $k_e f^2 B^2$ is the eddy current, and $K_a f^{1.5} B^{1.5}$ is the anomalous loss component. The loss per cycle is given by

$$W/f = k_h B^{\alpha} + k_e f B^2 + K_a f^{0.5} B^{1.5}. \quad (2b)$$

Equation (2b) can be compared to a quadratic equation of the type $a + bx + cx^2$ as shown in (2c), assuming that k_h, k_a, k_e, and α are constants that are independent of frequency and magnetic flux density. The coefficients of $f^{0.5}$ can be found by plotting a fitting curve

$$W = a + bf^{0.5} + cf \quad (2c)$$

where

$$a = k_h B^{\alpha} \quad b = k_a B^{1.5} \quad c = k_e B^2.$$

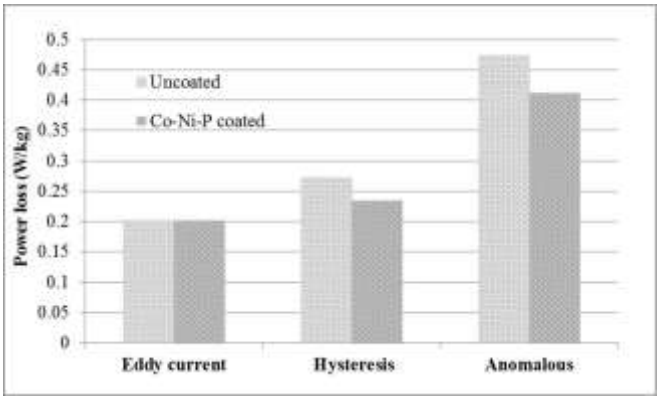

Fig. 11. Loss separation at 1.5 T magnetic flux density and 50 Hz frequency for the Co–Ni–P-coated sample at pH 9.

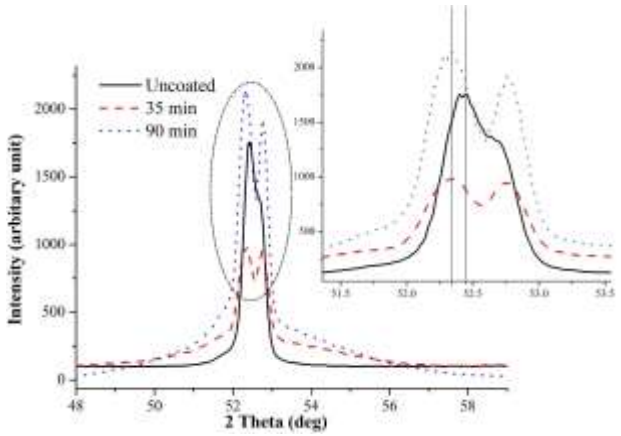

Fig. 12. XRD of the uncoated and Co–Ni–P-coated samples at pH 9.

The values were plotted over a range of frequencies from 10 to 1000 Hz to get a good approximation of the fitting. The value of the correlation coefficient [28] r^2 was 0.9997 and 0.99996 for the uncoated and Co–Ni–P-coated samples, respectively. Fig. 11 shows the loss separation data for the uncoated and coated samples. It can be clearly seen from the graph that the coated sample has a large reduction in anomalous loss, which is in agreement with the magnetic pattern viewer images.

H. X-Ray Diffraction

The XRD result in Fig. 12 shows the uncoated, 35-min and 90-min coated samples. The diffusive broad peaks in the histogram confirm the amorphous or nanocrystalline nature of the coating. The peaks may be Co–P or Co–Ni–P. The sharp peaks that were observed correspond to α-iron and α-iron-cobalt ($Fe_{0.3}Co_{0.7}$). The 110 reflection was shifted toward the lower angle in the coated sample, as can be seen in Fig. 12. Stress is introduced by the coating [22], which can expand the lattice of the substrate material.

The stress shift was interpreted from Bragg's law [29]. The shift in peaks toward a lower angle confirmed that the inter planer distance *d* increases and hence compressive stress developed in the coating. An equivalent tensile stress acted on the grain-oriented electrical steel surface to compensate the compressive residual stresses due to which there was an improvement in magnetic properties.

IV. Conclusion

An effective coating on grain-oriented electrical steel provides sufficient tension and insulation to reduce the specific total loss and magnetostriction. In addition to that, the magnetic activity and reduced thickness improves the stacking factor. An electroless deposition of Co–Ni–P was shown to provide an effective coating for electrical steels. The thickness of the coating was half the thickness of conventional coatings and being magnetic in nature, it further improves the stacking factor in the transformers to 98.83%. The threshold value of magnetostriction was shifted by 1.8 ± 0.20 MPa toward left after coating the sample. The time period for the electroless deposition dictates the thickness of the coating and hence the power loss reduction. A reduction of power loss by 4%–5% was observed for samples coated for 20 min as compared with a reduction of 9%–11% for samples coated for 90 min. The increase in pH of the solution from 7.8 to 9.0 decreases the surface roughness of the coating, which reduces the hysteresis loss. The domain structure was also narrowed, which reduces the anomalous loss; hence the overall total loss for grain-oriented electrical steel was reduced. It is suggested that these coatings could be scaled cost effectively to production material due to the simple autocatalytic process.

Acknowledgment

This work was supported by Tata Steel RD&T, Rotherham and Cogent Power Ltd., Newport.

References

[1] S. Turner, A. Moses, J. Hall, and K. Jenkins, "The effect of precipitate size on magnetic domain behavior in grain-oriented electrical steels," *J. Appl. Phys.*, vol. 107, no. 9, p. 09A307, 2010.
[2] J.-T. Park and J. A. Szpunar, "Effect of initial grain size on texture evolution and magnetic properties in nonoriented electrical steels," *J. Magn. Magn. Mater.*, vol. 321, no. 13, pp. 1928–1932, 2009.
[3] H. Haiji, K. Okada, T. Hiratani, M. Abe, and M. Ninomiya, "Magnetic properties and workability of 6.5% Si steel sheet," *J. Magn. Magn. Mater.*, vol. 160, pp. 109–114, Jul. 1996.
[4] J. W. Shilling, "Domain structure during magnetization of grain-oriented 3% Si–Fe as a function of applied tensile stress," *J. Appl. Phys.*, vol. 42, no. 4, pp. 1787–1789, 1971.
[5] C. R. Boon and J. A. Robey, "Effect of domain-wall motion on power loss in grain-oriented silicon-iron sheet," *Proc. Inst. Electr. Eng.*, vol. 115, no. 10, pp. 1535–1540, Oct. 1968.
[6] K. Tone, H. Shimoji, S. Urata, M. Enokizono, and T. Todaka, "Magnetic characteristic analysis considering the crystal grain of grain-oriented electrical steel sheet," *IEEE Trans. Magn.*, vol. 41, no. 5, pp. 1704–1707, May 2005.
[7] B. N. Filippov, S. V. Zhakov, and Y. G. Lebedev, "Influence of domain structure on some dynamic properties of ferromagnets," *IEEE Trans. Magn.*, vol. 15, no. 6, pp. 1849–1854, Nov. 1979.
[8] R. Langman, "The effect of stress on the magnetization of mild steel at moderate field strengths," *IEEE Trans. Magn.*, vol. 21, no. 4, pp. 1314–1320, Jul. 1985.
[9] T. Yamamoto and T. Nozawa, "Effects of tensile stress on total loss of single crystals of 3% silicon-iron," *J. Appl. Phys.*, vol. 41, no. 7, pp. 2981–2984, Jun. 1970.
[10] T. Olding, M. Sayer, and D. Barrow, "Ceramic sol–gel composite coatings for electrical insulation," *Thin Solid Films*, vols. 398–399, pp. 581–586, Nov. 2001.

[11] H. Yamaguchi, M. Muraki, and M. Komatsubara, "Application of CVD method on grain-oriented electrical steel," *Surf. Coat. Technol.*, vol. 200, no. 10, pp. 3351–3354, 2006.
[12] X. D. He, X. Li, and Y. Sun, "Microstructure and magnetic properties of high silicon electrical steel produced by electron beam physical vapor deposition," *J. Magn. Magn. Mater.*, vol. 320, nos. 3–4, pp. 217–221, 2008.
[13] G. O. Mallory and J. B. Hajdu, Eds., *Electroless Plating: Fundamentals and Applications*. FL, USA: American Electroplaters and Surface Finishers Society, 1990, ch. 4, pp. 121–122.
[14] P. Chivavibul, M. Enoki, S. Konda, Y. Inada, T. Tomizawa, and A. Toda, "Reduction of core loss in non-oriented (NO) electrical steel by electroless-plated magnetic coating," *J. Magn. Magn. Mater.*, vol. 323, nos. 3–4, pp. 306–310, 2011.
[15] D. M. Ionel, M. Popescu, S. J. Dellinger, T. J. E. Miller, R. J. Heideman, and M. I. McGilp, "On the variation with flux and frequency of the core loss coefficients in electrical machines," *IEEE Trans. Ind. Appl.*, vol. 42, no. 3, pp. 658–667, May/Jun. 2006.
[16] D.-H. Kim, K. Aoki, and O. Takano, "Soft magnetic films by electroless Ni-Co-P plating," *J. Electrochem. Soc.*, vol. 142, no. 11, pp. 3763–3767, 1995.
[17] P. I. Anderson, "Measurement techniques for the assessment of materials under complex magnetising conditions," *Electr. Rev.*, vol. 87, no. 9b, pp. 61–64, 2011.
[18] P. I. Anderson, A. J. Moses, and H. J. Stanbury, "Assessment of the stress sensitivity of magnetostriction in grain-oriented silicon steel," *IEEE Trans. Magn.*, vol. 43, no. 8, pp. 3467–3476, Aug. 2007.
[19] R. J. Taylor and J. A. Watt, "Magnetic pattern viewer," U.S. Patent 5 034 754, Jul. 23, 1991.
[20] A. A. Aal, A. Shaaban, and Z. A. Hamid, "Nanocrystalline soft ferromagnetic Ni–Co–P thin film on Al alloy by low temperature electroless deposition," *Appl. Surf. Sci.*, vol. 254, no. 7, pp. 1966–1971, 2008.
[21] A. K. Sharma, M. R. Suresh, H. Bhojraj, H. Narayanamurthy, and R. P. Sahu, "Electroless nickel plating on magnesium alloy," *Metal Finishing*, vol. 96, no. 3, pp. 10, 12, 14, and 16–18, 1998.
[22] J. Y. Song and J. Yu, "Residual stress measurements in electroless plated Ni–P films," *Thin Solid Films*, vol. 415, nos. 1–2, pp. 167–172, 2002.
[23] K. Parker and H. Shah, "The stress of electroless nickel deposits on beryllium," *J. Electrochem. Soc.*, vol. 117, no. 8, pp. 1091–1094, 1970.
[24] N. Fenineche, A. M. Chaze, and C. Coddet, "Effect of pH and current density on the magnetic properties of electrodeposited Co-Ni-P alloys," *Surf. Coat. Technol.*, vol. 88, nos. 1–3, pp. 264–268, 1997.
[25] T. Homma, J. Shiokawa, Y. Sezai, and T. Osaka, "*In situ* analysis of the deposition process of electroless CoNiP perpendicular magnetic recording media," in *Proc. Electroechem. Soc.*, 1995, pp. 181–190.
[26] K. S. Lew, M. Raja, S. Thanikaikarasan, T. Kim, Y. D. Kim, and T. Mahalingam, "Effect of pH and current density in electrodeposited Co–Ni–P alloy thin films," *Mater. Chem. Phys.*, vol. 112, no. 1, pp. 249–253, 2008.
[27] T. Wada, T. Nozawa, and T. Takata, "Method for producing a super low watt loss grain oriented electrical steel sheet," U.S. Patent 3 932 236, Jan. 13, 1976.
[28] R. A. Fisher, "Frequency distribution of the values of the correlation coefficient in samples from an indefinitely large population," *Biometrika*, vol. 10, no. 4, pp. 507–521, May 1915.
[29] W. L. Bragg, "The diffraction of short electromagnetic waves by a crystal," in *Proc. Cambridge Philos. Soc.*, vol. 17. 1913, pp. 43–57.